Nuclear Instruments and Methods in Physics Research A 840 (2016) 113–120

Contents lists available at ScienceDirect

Nuclear Instruments and Methods in Physics Research A

journal homepage: www.elsevier.com/locate/nima

Inverse Compton scattering X-ray source yield optimization with a laser path folding system inserted in a pre-existent RF linac

A. Chaleil[a,*], V. Le Flanchec[a], A. Binet[a], J.P. Nègre[a], J.F. Devaux[a], V. Jacob[a], M. Millerioux[a], A. Bayle[a], P. Balleyguier[a], R. Prazeres[b]

[a] CEA DAM DIF, F-91297 Arpajon, France
[b] CLIO/LCP, Bâtiment 201, Université Paris-Sud, F-91450 Orsay, France

ARTICLE INFO

Keywords:
Inverse Compton scattering
Compact light source
Electron linac
X-ray sources

ABSTRACT

An inverse Compton scattering source is under development at the ELSA linac of CEA, Bruyères-le-Châtel. Ultra-short X-ray pulses are produced by inverse Compton scattering of 30 ps-laser pulses by relativistic electron bunches. The source will be able to operate in single shot mode as well as in recurrent mode with 72.2 MHz pulse trains. Within this framework, an optical multipass system that multiplies the number of emitted X-ray photons in both regimes has been designed in 2014, then implemented and tested on ELSA facility in the course of 2015. The device is described from both geometrical and timing viewpoints. It is based on the idea of folding the laser optical path to pile-up laser pulses at the interaction point, thus increasing the interaction probability. The X-ray output gain measurements obtained using this system are presented and compared with calculated expectations.

1. Introduction

Several Inverse Compton Scattering (ICS) projects have arisen around the world to meet the demands for X-ray production in the various fields of research and applications such as cultural heritage, imaging, and cancer therapy [1]. The Compton scattering process can be used to develop X-ray sources from the interaction between a visible laser beam and a multi-MeV electron beam. Though the peak X-ray brightness of such sources is lower than what can be obtained from high-brightness sources such as synchrotrons or free-electron lasers, they have several advantages. For example, inverse Compton scattering sources provide X-ray photons at a tunable energy in a broad spectral range that can be easily extended beyond 100 keV. The building cost and size are comparatively smaller, making them potentially affordable for more laboratories and for medical centers. At the CEA (Commissariat à l'Energie Atomique et aux Energies Alternatives) of Bruyères-le-Châtel, the characterization of high-speed hard X-ray detectors requires 30 ps pulses, tunable from 10 to 60 keV, to be delivered in single-shot mode for impulse response measurements. To address this specific need, an ICS source was developed on the ELSA accelerator (Electrons, Laser, X-ray Sources and Applications) at the CEA [2]. In 2011, the results from the first Compton experiment on ELSA demonstrated its feasibility with a 17 MeV electron beam and 532 nm laser pulses [3]. The electron and laser bunches were emitted at a frequency of 72.2 MHz during 2 μs trains, called macro-pulses. The average flux obtained in a 25 mrad half-angle cone was $1.2{\cdot}10^4$ pH/s with a maximum energy of 11 keV. These preliminary results led us to establish the first dimensioning for the future evolution of the source set up, to improve the X-ray photon flux and to make it routinely available for scientific users.

Increasing the X-ray photon flux on ICS facilities most often relies on the recirculation of electrons or photons, making them recurrently available for new collisions. For instance, an electron storage ring has been developed by Lyncean Technologies Inc. in California (USA) [4] Technical University Munich (TUM) has started using routinely a Lyncean Technologies source since April 2015 [5]. The THOMX project, currently under development in France, uses the same concept of electron recirculation in a storage ring [6–8]. In these two schemes, photons are also recirculating in order to increase the number of photons involved in the Compton diffusion process: a high average laser power (~160 W) is stored in a very high finesse (typically 30,000) Fabry-Perot cavity [9]. This technology is based on phase coherent addition of laser waves [10–12], which involves feedback systems ensuring high precision mirror positioning. Resonant systems are particularly well suited for recurrent operation: the phase coherent addition of several tens of thousands laser picosecond pulses, allowing the multiplication of interactions, is obtained thanks to the high temporal coherence of a mode-locked oscillator in continuous wave (cw) mode. Another approach consists in using a non-resonant optical circulator with fewer optical passes. For example, a specific non-

* Corresponding author.

http://dx.doi.org/10.1016/j.nima.2016.10.008
Received 25 July 2016; Received in revised form 22 September 2016; Accepted 3 October 2016
Available online 06 October 2016

resonant circulator using two fixed large diameter parabolic mirrors facing each other and a mirror-pair system is under development at LAL [13] in the framework of the European Extreme Light Infrastructure project dedicated to Nuclear Physics (ELI-NP-GS) [14–16]. In this paper, we present a different non-resonant optical folding system based on the use of two sets of seven small spherical mirrors evenly spread on two flat plates placed upstream and downstream the interaction point. We show that, though the idea of recirculation is intuitively associated with a recurrent mode of operation, it can indeed be used to increase the number of visible photons meeting one single electron bunch, therefore allowing single-shot applications like impulse response measurements. In the case of single-shot mode, which is our main focus in this development, phase locked addition of resonant systems in cw mode and the complexity of sub-nanometer mirror positioning is not necessary. High gain laser amplifiers are used to produce high energy pulses during a few tens of microseconds, only limited by the damage threshold of optical elements. Our system allows overcoming this limitation, by piling up eight pulses at the interaction point, with typical longitudinal positioning tolerances of 10 µm. It is worth mentioning that it can also be used in a recurrent set-up, in which each laser pulse meets several successive electron bunches. In the remainder of this paper, the experimental set-up is described, measurements of the X-ray output gain obtained in the recurrent mode are presented, and experimental results are then compared with calculated expectations.

2. ELSA Compton source

The ELSA facility is based on an RF electron linac providing a high quality and low emittance electron beam [17,18]. 34-ps electron bunches, extracted from a photocathode by a laser system, are accelerated in a 144 MHz RF cavity, then in three 433 MHz cavities (Fig. 1). Ultra-short quasi-monochromatic X-ray pulses are produced by inverse Compton scattering in a dedicated area where 17,7 MeV electron bunches meet 34-ps laser pulses synchronously emitted at a 532 nm wavelength.

The ICS principle is described in Fig. 2. In our setup, θ_1 is close to 180°. The incident photon energy is negligible compared to the electron rest energy. If placed in the laboratory frame, the energy change of the electron after one scattering event is negligibly small, while the energy of the backscattered photon is increased by a factor $4\gamma^2$ due to a double relativistic Doppler effect (where γ is the Lorentz factor). This can be easily demonstrated by calculating the frequency shift of scattered photon after two successive changes of the reference frame. The energy of the X-ray photons is proportional to the visible photon energy (typically 2.5 eV for a 532 nm photon) and to the square of electron kinetic energy (17,7 MeV in our experiments).

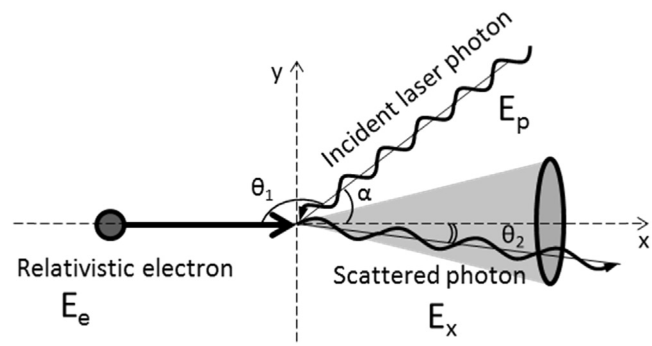

Fig. 2. Inverse Compton scattering scheme also called Compton backscattering.

Table 1
Experimental setup for of the recent inverse Compton source developed in 2015.

1. Parameters of the electron beam	
Kinetic energy of electrons	17.7 MeV
Macro-pulse duration	2.9 µs
Current in the macro-pulse	25 mA
Micro-pulse rms duration	34 ps
Micro-pulse charge	0.4 nC
Normalized rms horizontal emittance	7.8 µm rad
Normalized rms vertical emittance	18.9 µm rad
Rms transverse radius	105 µm(h)
	73 µm(v)
2. Parameters of the laser beam	
Laser wavelength	532 nm
Macro-pulse duration	1.8 µs
Micro-pulse rms duration	34 ps
Energy in one macro-pulse	65 mJ
Energy in one micro-pulse	0.5 mJ
Rms transverse radius	84 µm(h)
	64 µm(v)
3. Parameters of the new X-ray source	
X-ray energy	11 keV
Number of interaction per second	130
Average light flux with SMILE (in a 10 mrad half-angle cone)	2.9 10^4 ph/s
Peak light flux (in a 10 mrad half-angle cone)	3.2 10^{12} pH/s

The accelerator and the Compton source parameters are detailed in Table 1.

An estimated number of emitted photons per time unit is given by [19]:

$$\frac{dN_X}{dt}=\sigma_{Th}L \tag{1}$$

where σ_{Th} is the Thomson cross section ($\sigma_{Th}=\frac{8}{3}\pi r_e^2=6.\ 652\cdot10^{-29}$ m² with

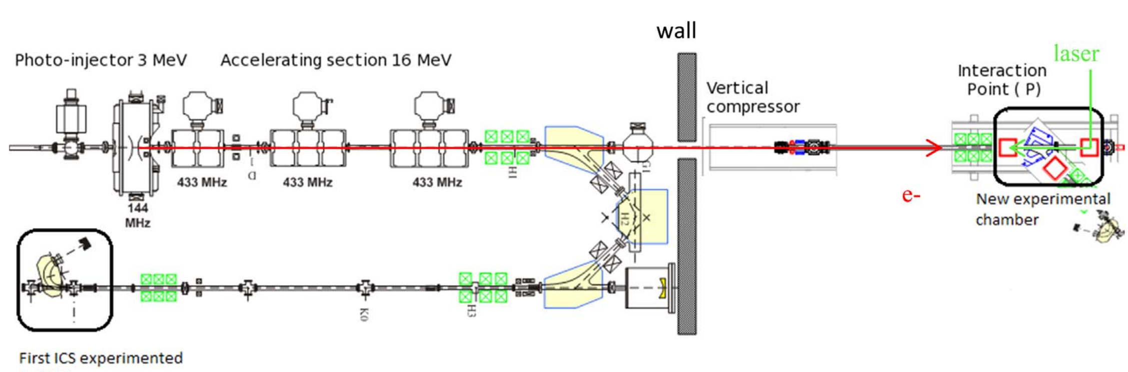

Fig. 1. Schematic upper view of ELSA linac (to the left of the wall) with the new ICS chamber placed at the end of the experimental beamline (to the right of the wall). Electrons are extracted from a photocathode, using the photoelectric effect, and exit the photo-injector with a maximal energy of 3 MeV. Electrons pass through three RF cavities, in which the frequency of the electromagnetic field is 433 MHz, to reach a maximum energy value of 19 MeV. At the end, electron bunches are guided to the interaction point for inverse Compton Scattering experiments. The red arrow shows the beam direction. The beam line after the U-turn, in which 2011 ICS experiments were done, is no longer used. (For interpretation of the references to color in this figure legend, the reader is referred to the web version of this article.)

r_e the classical radius of electron), and L is the luminosity in pH/s/m^2, defined in the case of two Gaussian beams by the expression [20]:

$$L = \frac{N_e N_p f_{rep} \eta}{2\pi\sqrt{\sigma_{ye}^2 + \sigma_{yp}^2}\sqrt{(\sigma_{ze}^2 + \sigma_{zp}^2)\sin^2(\frac{\alpha}{2}) + (\sigma_{xe}^2 + \sigma_{xp}^2)\cos^2(\frac{\alpha}{2})}} \tag{2}$$

In this expression, N_p is the number of photons in the incident laser pulse, N_e the number of electrons in the bunch, f_{rep} the repetition rate of the bunches, $\alpha = \pi - \theta_1$, $\sigma_{(y,z)i}$ the *rms* transversal beam size of incident electron (i=e) and photon (i=p) bunches and σ_{xi} the longitudinal beam size at the interaction point. The η factor takes into account the overlapping of the beams.

As a general rule, the source efficiency will be optimized with θ_1 as close as possible to 180°, and L as large as possible. This can obviously be achieved by reducing the bunch sizes at the interaction point. However, the laser focusing is limited by diffraction and the electronic bunch current density is limited by space charge effects. The highest manageable charge in ELSA with a good normalized *rms* emittance (less than 10 µm rad after passing through the alpha magnets of our compressor [21]) is roughly 2 nC for a 30 ps-bunch. The laser pulse energy is limited to 100 µJ, which is determined by the damage threshold of the Nd:YAG amplifier and of the optical lenses surfaces. Several laser pulses of typically 100 mJ can be emitted, but not simultaneously, to avoid damaging the surfaces.

In the case of single shot applications, the X-ray pulse has to be emitted from one single electron bunch. To increase the photon density at the interaction point, we pile-up successive laser pulses at the interaction point by folding the laser optical path in a geometrical 3D-arrangement: laser pulses arrive exactly at the same time at the interaction point, to meet the single electron bunch for Compton interaction. In this arrangement, a single X-ray pulse is emitted, which is needed for our applications, but the number of X-ray photons is roughly multiplied by the number of laser passes through the optical system. This system named SMILE (System of Multipass optical beam for Interaction between Laser and Electrons) will be detailed in the next part of this article.

Furthermore, our system can be used in a recurrent mode. When emitting several hundreds of successive electron bunches and laser pulses, each laser pulse interacts with an electron bunch each time it passes through the interaction point. The results presented in this paper were experimentally obtained in this latter setup, which makes measurements easier.

3. Experimental setup

3.1. SMILE description

The SMILE system consists of two sets of seven spherical mirrors circularly distributed around the electron beam axis (Fig. 3). The sets face each other on both sides of the interaction point P. The curvature radius of the spherical mirrors has been calculated such that the beam waist is located in the interaction plane each time the laser beam travels from one set to the other. Taking into account typical electron beam emittance and laser beam diffraction, both particle beams are expected to have a 1/e^2 dimension of 100 µm at the interaction point. The laser beam radius (1/e^2 value) on the spherical mirrors is then 1.75 mm for the laser wavelength of 532 nm. Spherical mirrors of 9 mm diameter are thus sufficiently large to reflect the whole beam. Taking the size of the mirror holding systems into consideration, 7 mirrors of 9 mm diameter can be fitted on both sets of SMILE. The mirrors centers are located 13 mm from the electron trajectory axis, allowing all laser beam folded trajectories to fit inside a 55 mm diameter vacuum pipe. Each mirror set has a 20 mm diameter central hole. The electrons enter the system through the hole of the first set (Set 1) while the X-rays exit the system through the hole of the second set (Set 2). The laser photons enter through a smaller off-axis hole of the second set, also located 13 mm from the electron trajectory axis. The laser beam meets the electron beam with a collision angle α of about 30 mrad.

The laser beam enters the SMILE system after being reflected by the 45° tilted mirror of the injection unit (Fig. 4). It travels through the entrance hole of Set 2 to reach the interaction point P. It is then reflected by the M_1 mirror of Set 1 toward M_2 mirror of Set 2. Since M_2

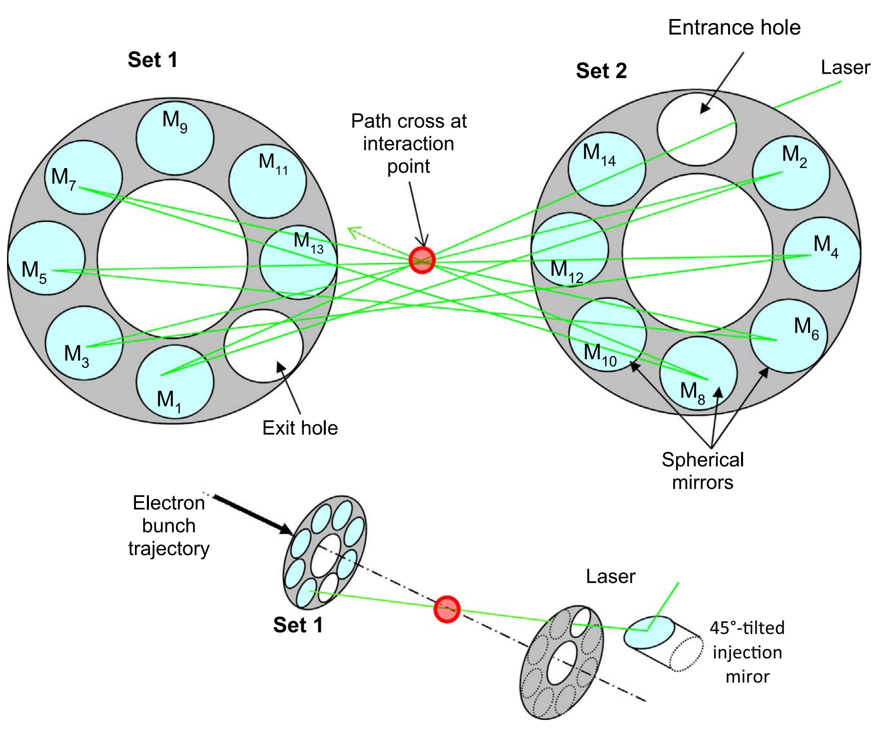

Fig. 3. Laser and electron paths in the SMILE system. The electron beam enters through the central aperture in the Set 1 and the laser beam is injected in SMILE thanks to a 45°-tilted mirror placed behind the Set 2.

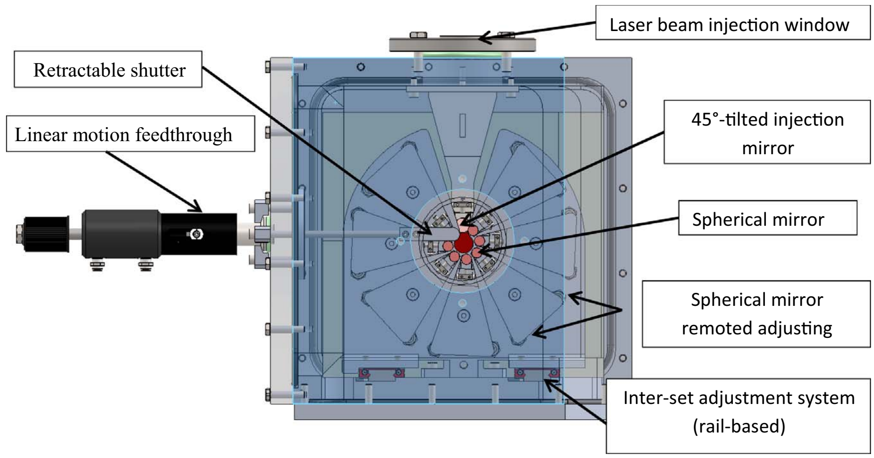

Fig. 4. Enlarged view of injection unit. Retractable shutter managed by a linear motion feedthrough. The mirror M2 is hidden by the shutter to avoid the beam path folding in the SMILE system. In this case, only one laser pulse interacts with the electron bunch.

azimuth is shifted by 45° with respect to the entrance hole, the trajectory from M_1 to M_2 does not cross the interaction point P. Instead, the beam is reflected by M_2 toward M_3 to cross P for the second time. It is then reflected back toward Set 2 and so on, until it exits the system through the exit off-axis hole of Set 1.

With 7 mirrors and one hole, in recurrent mode, 8 pulses are piled-up at the interaction point at the working frequency of 144 MHz. In the stationary regime (with 130 bunches per 1.8 µs macro-pulse, we neglect the start and the end effect of these trains in the photon count), the theoretical gain expected on the X-ray yield is 8. In single shot mode, on the other hand, 8 laser pulses are used for only one electron bunch. The electron bunch is sent to the interaction point when the 1st photon pulse has travelled 8 times through the SMILE system, the 2nd pulse has travelled 7 times, the 3rd pulse 6 times, and so on, until the arrival of the 8th pulse at the interaction point. As a result, a single X-ray pulse is produced, with 8 times more photons than without SMILE. This is a valuable tool since the energy of each photon pulse is limited by the damage threshold of optical surfaces.

The distance between the two mirror sets is adjusted with the rail system placed below Set 2 (Fig. 4), so that the round-trip duration matches the time between two laser pulses. Precise measurements of the 8 laser pulses synchronization are done by a streak camera. In single shot mode, the choice of laser frequency is theoretically free, since only one electron bunch is used. But to ensure the synchronization of typically within 1 ps, it is convenient to use a mode-locked laser, with a feedback system locked to the base frequency of the RF accelerator, or a multiple of this frequency. In the recurrent mode, both electrons and photons must share the same repetition rate to get the maximum number of interactions. On ELSA, all our synchronization systems are based on the same frequency synthesizer at 72.2 MHz. Though the usual repetition frequency of the electron bunches is 72.2 MHz, the accelerator can potentially be used either at 72.2 or 144.4 MHz. At 144.4 MHz, the distance between the two sets of SMILE should be 1038 mm. At 72.2 MHz this distance would be 2076 mm, which would make the system more prone to geometric instabilities. To accommodate the SMILE length to the ELSA experimental beamline, the 1038 mm SMILE configuration was chosen, though the laser we had at the time of the experiment was of 72.2 MHz. In order to test our

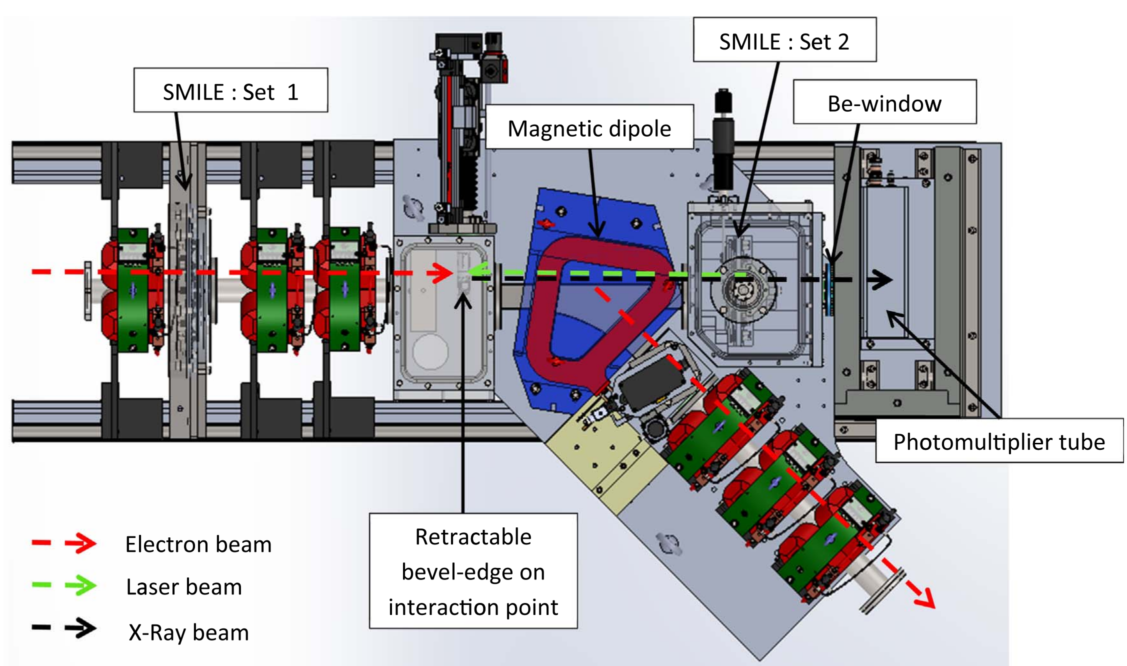

Fig. 5. Top view of the new Compton experimental chamber with electron, laser, and X-rays beam trajectories. (For interpretation of the references to color in this figure, the reader is referred to the web version of this article.)

system in the routinely operating conditions, two experiments, which differ only in the electron bunches repetition rate, were carried out. Implications for the experimental results using the SMILE system, are carefully taken into account and thoroughly explained in the next section.

In order to measure SMILE efficiency, we included in our experimental set-up a retractable shutter in front of M_2 mirror (Fig. 4). The optical path is cut after the first laser pass through the interaction point, so that the laser beam can be used either once or eight times, depending on the position of a pneumatic linear motion feedthrough.

3.2. Experiment description

Following our first experiments using inverse Compton scattering in 2011, a new chamber set was designed (with AVANTIS Engineering Group) to move the ICS source to a more suitable place on ELSA beam lines. New electron guiding elements were also designed and installed with all detection systems required for optimizing the source (temporally as well as spatially). This new chamber set mainly consists of three units. The first is the interaction unit where the Compton scattering takes place. The second is the injection unit used to inject the laser toward the interaction point and through which the X-rays are extracted. The third is the spectrometer unit placed after the electron beam deviation, once it has gone through the interaction point.

The technical drawing shows a top view of the chamber (Fig. 5). The electron beam travels from left to right as shown by the red dashed arrow. It is focused by a magnetic quadrupole triplet to the interaction point. The laser beam is focused by a multiple-lenses optical system (not shown on the drawing) allowing the adjustment of the beam waist position and width, prior to entering the injection unit through a glass-window. The beam is directed by the off-axis 45°-tilted mirror toward the interaction point (dashed green arrow). X-rays leave the unit in the same direction as the incident electron beam through a 200 µm-thick Beryllium (Be)-window (typically 98% transmission at 11 keV). After interaction, the divergent electron beam is deviated by a dipole magnet and focused by a second triplet of quadrupoles toward an electron beam-dump.

Two diagnostics are needed to check the spatial and temporal bunch overlap (Fig. 6). An aluminum retractable bevel-edge is placed at the interaction point. It is impacted by the electron beam on the left side and by the laser beam on the right side. The electron beam position is visualized thanks to the optical transition radiation (OTR) from the bevel-edge surface. The position of the bevel-edge is adjusted so that both beams are as close to the edge as possible. To optimize the transverse overlap, an image of the impact of both beams is formed by an optical lens onto a CCD camera. The electron beam focusing point is adjusted with respect to the laser focus point so that they are exactly symmetric about the edge. The spatial overlap is thus ensured when the bevel-edge is removed from the interaction point.

Both OTR and laser light are also transmitted to a streak camera thanks to a semi-transparent mirror (Fig. 6). Typical images of our streak camera show the trace of both electron and photon signals acquired simultaneously. Time is measured on the vertical axis. Photons and electrons arrive simultaneously when both traces are horizontally aligned. Fine adjustments are performed by shifting the mode-locked laser timing reference signal with respect to the RF electron phase in the accelerator.

In this study, two X-ray measurement systems are used. Measurements consists of an already published setup [19] where the spontaneous fluorescence signal released by an irradiated Image Plate (IP) (Fujifilm BaFBr:Eu2+) tilted at 45°. In the first measurement system, the fluorescence signal is amplified and converted into electric signal by a photomultiplier tube. This system was mainly used to monitor interaction during beam adjustments but it is not precise enough to provide reliable quantitative measurements. The second measurement system is based on X-ray accumulated dose on a single IP after several shots (lasting typically 2 min at 1 Hz). It provides 2D images of the X-ray source similar to those shown in our previous paper [3]. After corrective post-treatment including background noise subtraction, and taking into account the emitted X-ray spectrum, the number of X-ray photons produced by interaction can be estimated with accuracy at the level of tens of photons compared to the simulation study. Thus, the value of the X-ray photon flux given in this paper is an approximate estimation of the real X-ray flux produced.

The SMILE system was developed and tested in the course of 2015. Two experiments were conducted which differ in the electron bunch repetition rate. The temporal sequence of the successive experiments is detailed in Fig. 7.

The first one involved both 72.2 MHz electron and laser beams (Fig. 7a). Given the fact that the SMILE system is based on a frequency

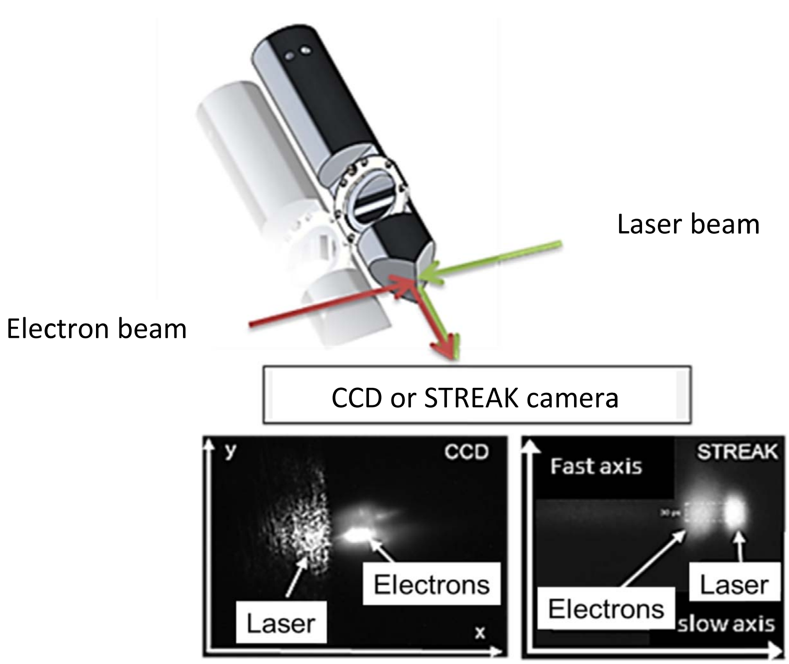

Fig. 6. Spatial and temporal diagnostics for overlap adjustments on the bevel-edge.

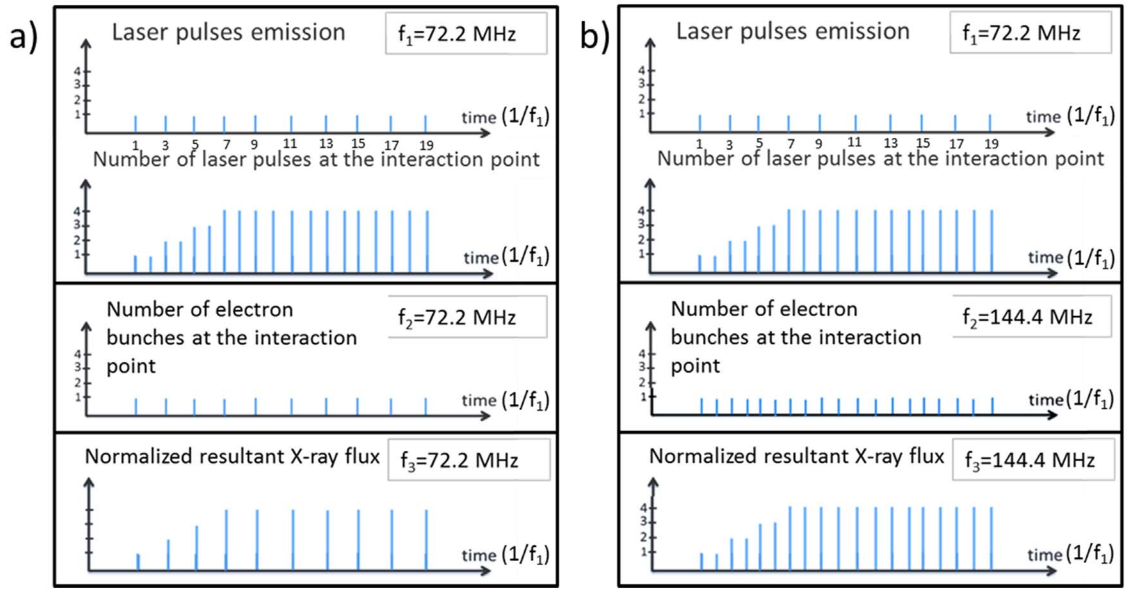

Fig. 7. Temporal sequence of particle bunches at the interaction point with SMILE in the first experiment (a) and in the second experiment (b). The laser pulses used for interaction are generated at a 72.2 MHz frequency but the SMILE system piles-up laser pulses on the interaction point with at its working frequency f1=144.4 MHz. Electron bunches are emitted at a frequency f2 which is 72.2 or 144.4 MHz. The frequency of X-ray generation f3 is doubled when passing from the first to the second experiment.

of 144.4 MHz, it takes two round-trips to pile a laser pulse with the next one at the interaction point (instead of 1 in case of 144.4 MHz). In the stationary regime, each laser pulse interacts with 4 electron bunches before it exits. So we expected a gain of 4 on the X-ray flux. The beam parameters of the first experiment are listed in Table 1.

In the second one, we doubled the electron bunches repetition rate to 144.4 MHz while the laser pulse emission frequency was kept unchanged. We could produce a 144.4 MHz electron beam by modifying the photo-injector system of the accelerator. The 72.2 MHz laser beam used to extract electrons from the photo-cathode was split in two contributions, one path being delayed with respect to the other before impacting the photo-cathode. By finely adjusting the delay between those two paths, we could illuminate the photo-cathode at 144.4 MHz. Thus the charge of each electron bunch is divided by two. However, as the number of electron bunches per second is doubled, the current remains constant.

Here, the laser pulses involved in the Compton interaction are still emitted at 72.2 MHz (the frequency doubling was not possible to apply to this laser), while the electron bunches have a 144.4 MHz frequency (Fig. 8b). Each laser pulse meets 8 electron bunches. Such an

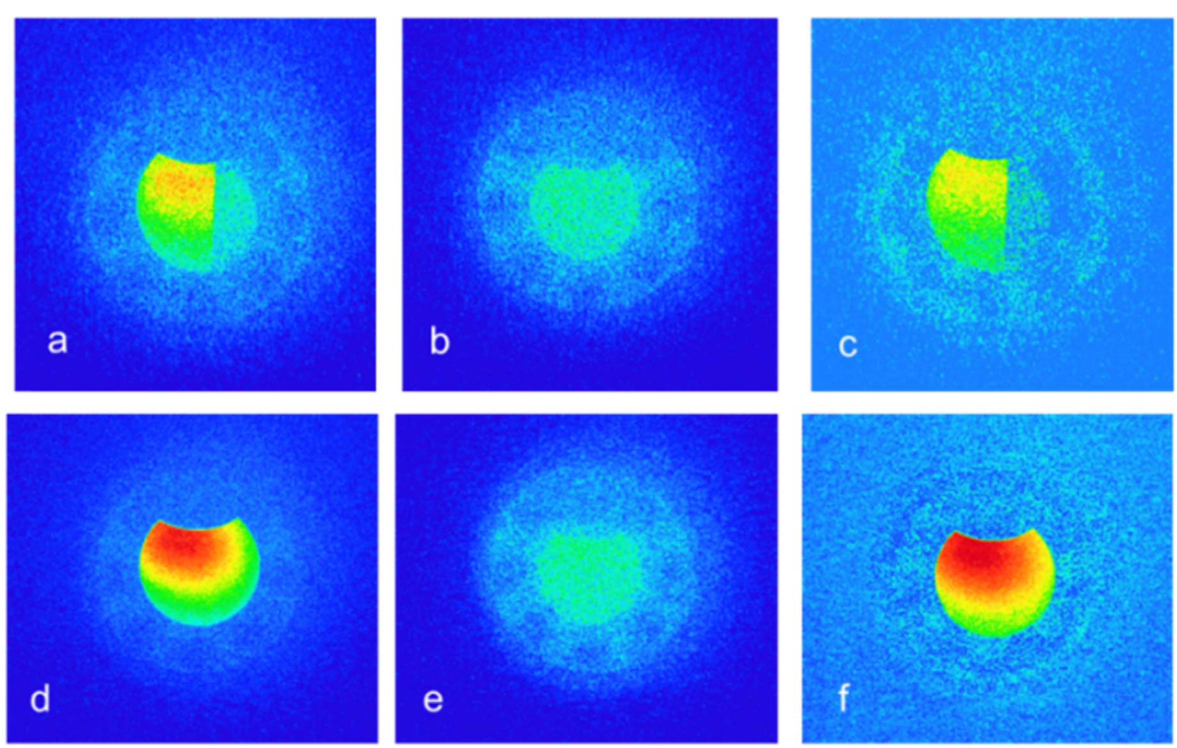

Fig. 8. X-ray images extracted from image plates. The images of the first row (a)–(c) are obtained without SMILE. Images of the second row (d)–(f) are obtained whith SMILE. In both cases, images show ICS signal and noise (a), (d), background noise (b), (e), and extracted ICS signal (c), (f). SMILE is turned off by a retractable shutter designed to hide the first mirror of the SMILE system. On the images (a) and (c), the edge of the retractable shutter can be seen.

experiment was needed to verify the efficiency of each of the 8 passes of the laser pulse at the interaction point, comparing to 4 in the first experiment. By doubling the number of interactions per second, we expected doubling the gain on the X-ray flux from 4 to 8. However, during all our inverse Compton experiments, we ensured that the current remained constant. We can conclude that the gain on the X-ray photon production per interaction is also 4..

3.3. Results

IP images are used to evaluate the number of produced ICS X-ray photons. Those obtained in the first experiment with both electron bunches and laser beam emitted at 72 MHz are presented in Fig. 8a–c. The imager gives the intensity of each pixel from an image array in the arbitrary PSL (PhotoStimulated Luminescence) unit. The cumulative dose is then expressed in PSL/mm^2. The corresponding amount of photons is obtained applying the correction factor related to the absorption of X-ray radiations by the different media (Be or air) and to the IPs' sensitivity which is a function of the scattered energy [19]. All experimental results of flux (expressed in photons per second) are calculated from integrating photon numbers over the surface subtending a chosen angle, divided by the irradiation time of the IP.

We first measure the cumulative dose on images from the IPs to extract the related Signal to Noise Ratio (SNR). The background noise is mainly due to the Bremsstrahlung radiation produced by electrons in the halo when they interact with the vacuum pipes. The laser pulses piling at the interaction point improves the ICS signal but leaves the noise level unchanged. The SNR obtained from the images shown in Fig. 8, is about 2 without the SMILE improvement (Fig. 8a–c) to be compared against 11.2 with the SMILE improvement (Fig. 8d–f). The photon yield multiplication factor directly measured from PSL level is ~5.6. The difference with the theoretical gain value of 4 could be related to the repeatability of the experimental parameters including beam positioning and experimental errors of flux calculations. In addition, the impact of SMILE on the X-ray photon yield is measured using a retractable shutter cutting the optical path after the first laser pass through the interaction point. Thus, the difference could also be explained by the beam misalignment that degrades progressively as the beam passes multiple times resulting in an overestimation of the gain. All these results show that the SMILE system significantly improved the signal to noise ratio.

With regards to the emitted flux, we expected to produce a total flux without SMILE of $1.4\bullet10^4$ pH/s in a 10 mrad half-angle cone according to Eq. (2). The recent results of the current source have shown an average X-ray flux of $4.1\bullet10^3$ pH/s in the referential 10 mrad half-angle cone and $1.1\bullet10^4$ pH/s in the 25 mrad half-angle cone. As not all the interaction parameters are taken into account in the analytical calculation, the theoretical value of flux is considered to be a rough estimate of experimental X-ray photon yield. The difference by a factor of 3 with the effective flux produced in experiment can be explained, among other reasons, by angle and beam size measurement error at the interaction point, by the fluctuations in beams transport and by X-ray photons measurement error related to detecting conditions and background noise.

The flux provided by the source benefiting from the SMILE improvement (Fig. 8f) is $2.2\bullet10^4$ pH/s integrated over the 10 mrad half-angle cone and $6.0\bullet10^4$ pH/s in the 25 mrad half-angle cone.

The source profile produced with and without SMILE in this experiment is shown in Fig. 9. This figure shows a good agreement between the 2015 and the 2011 profiles. The profile width obtained with SMILE is very similar to that of the source produced without SMILE. Although the optical axes of the 8 incoming pulses are not contained in the same incidence plane, the collision angle is kept constant; indeed, no increase in the scattering angle is observed. The 8 simultaneous X-ray beams are still emitted in the same direction; i.e., the electron propagation axis. This result demonstrates the low sensitivity of scattering angle when SMILE is operating: the X-ray direction of emission is defined by the electron beam axis.

The results obtained in the second experiment are presented in this paragraph. The waveforms acquired from the photomultiplier tube in this configuration, using a 144.4 MHz electron beam, are shown in Fig. 10. The ICS waveforms acquired when SMILE is turned on and off are compared. Such a qualitative *in situ* measurement is only used to detect an increase of the signal. It cannot be used as a quantitative diagnostic because the photomultiplier could not be precisely positioned from a geometrical viewpoint. Moreover, the time response of this diagnostic is much longer than one micro-pulse. To make more precise measurements, we have to work out the number of X-ray photons on the images of the source. X-ray signals were measured after successively occulting one of the two photo-injector laser contributions to the electrons extraction from the photo-cathode to produce 144.4 MHz electron bunches. Each contribution is expected to produce a 72.2 MHz electron beam. Experimentally, the flux improvement independently obtained with SMILE by each 72.2 MHz beam contribution is roughly half of the total improvement obtained by the resultant 144.4 MHz electron beam, which gives a confirmation that the total improvement is well distributed among all the 8 laser pulses.

Regarding the photon numbers, the flux obtained in the 10 mrad half-angle cone is $2.9\bullet10^4$ pH/s, namely a gain of 7.0 in comparison with the $4.1\bullet10^3$ pH/s provided by the initial source without the SMILE improvement. However, regarding the flux in the total 25 mrad half-angle that reaches $8.8\bullet10^4$ pH/s and the gain rises to 8.0 compared to $1.1\bullet10^4$ pH/s. As one laser pulse interacts 8 times, which is twice the first experiment value, an 8-fold gain is expected on the initial source flux.

These results demonstrate the profitable impact of SMILE on the source performance.

4. Conclusion and prospects

The improvement in flux obtained by using the optical folding system SMILE in the new ELSA ICS experimental chamber was confirmed by our first measurements of X-rays produced with a 17 MeV electron beam and a 532 nm laser beam. The technological choices were validated including the overall configuration of the SMILE system. The measurements of the flux obtained in two experiments allowed us to evaluate the gain provided by SMILE with respect to the number of emitted X-ray photons. In the first experiment, each electron bunch interacted with four laser bunches. The related gain

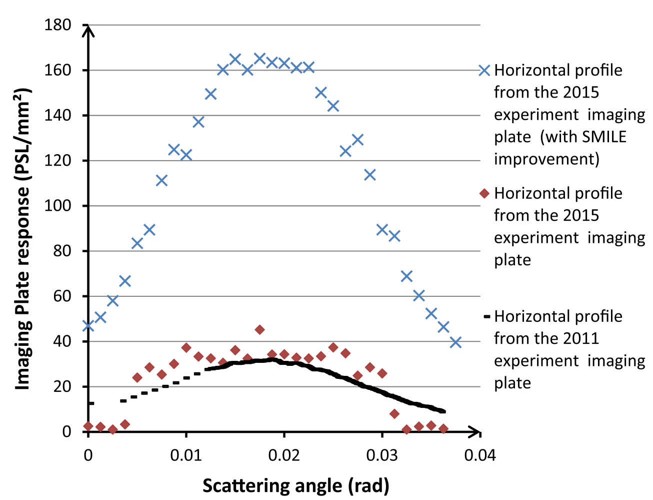

Fig. 9. Angular distribution of the radiation spectrum directly extracted from imaging plates of Fig. 10. Imaging plates response to the X-ray source produced in 2011 (green dots) is compared with the 2015 results obtained without SMILE (red dots) and with the SMILE (blue dots). (For interpretation of the references to color in this figure legend, the reader is referred to the web version of this article.)

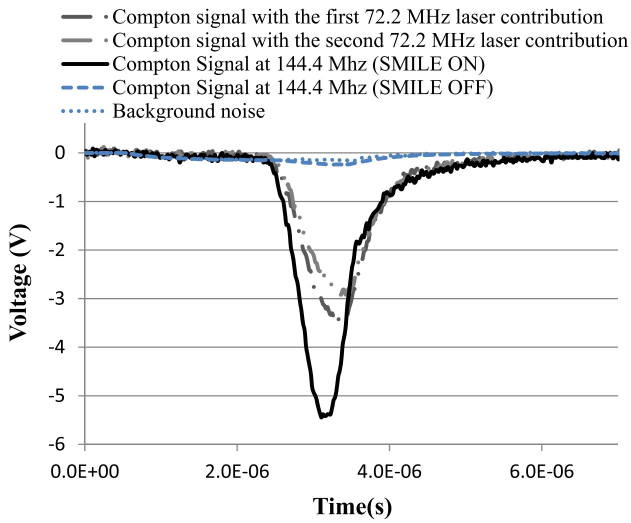

Fig. 10. X-ray signals emitted during one macro-pulse of 2 µs. The electrical signals acquisition is performed through the photomultiplier tube. The gain of the Compton signal at 144.4 MHz is compared to the two 72.2 MHz contributions show the efficiency of the frequency-doubling.

has reached the expected theoretical gain of 4 and the scattering angle has not been modified compared with a similar experiment without using SMILE. In the second experiment, the number of interactions per second has been doubled and the expected gain of 8 was fulfilled again.

Thanks to the SMILE system the ELSA inverse Compton source benefits from a gain of 8 on the X-ray yield in the recurrent working mode as much as in the single-shot mode. As a result, the signal to noise ratio in experiment with SMILE is significantly improved and the X-ray detection is considerably facilitated.

A facility upgrade is in progress [21] at the ELSA linac to raise the electron energy from 17 to 37 MeV in order to provide additional gain. With such an increase, the geometrical emittance will be improved, and the halo reduced. This, in turn, should lead to a decrease of the residual noise. First experiments in the single shot mode will be carried out in 2016.

References

[1] P. Walter, A. Variola, F. Zomer, M. Jaquet, A. Loulergue, Comptes Rendus Phys. 10 (2009) 676.
[2] J.L. Lemaire, in: Proceedings of the International Linear Accelerators Conference, JACoW, Lübeck, Germany, 2004, pp. 153–155
[3] A.S. Chauchat et al., in Proceedings of International Particle Accelerator Conference, JACoW, New Orleans, Louisiana, USA, THPPR042, 2012, pp 4068–4070
[4] M. Bech, O. Bunk, C. David, R. Ruth, et al., J. Synchrotron Rad. 16 (1) (2009) 43–47.
[5] E. Eggl, et al., J. Synchrotron Rad. 23 (5) (2016) 1137–1142.
[6] A. Variola, in: Proceedings of 2nd International Particle Accelerator Conference, JACoW, San Sebastian, Spain, WEOAA01, 2011, pp 1903–1905
[7] C. Bruni, J. Haissinski, A. Loulergue, R. Nagaoka, in: Proceedings of 2nd International Particle Accelerator Conference, JACoW, San Sebastian, Spain, MOPS050, 2011, pp. 715–717
[8] I.V. Drebot et al., in: Proceedings of the 4th International Particle Accelerator Conference, JACoW, Shanghai, China, MOPWO004, 2013, pp. 888–890
[9] J. Bonis et al., IOP publishing for SISSA, JINST 7 P01017, 2012
[10] T. Akagi, et al., Nucl. Instrum. Methods A 724 (2013) 63–71.
[11] F. Zomer, Y. Fedala, N. Pavloff, V. Soskov, A. Variola, Appl. Opt. 48 (35) (2009) 6651–6661.
[12] V. Brisson, et al., Nucl. Instrum. Methods A 608 (1) (2009) S75–S77.
[13] K. Dupraz, et al., Phys. Rev. ST Accel. Beams 17 (2014) 033501.
[14] C.A. Ur, D. Balabanski, G. Cata-Danil, S. Gales, I. Morjan, O. Tesileanu, D. Ursescu, I. Ursu, N.V. Zamfir, Nucl. Instrum. Methods B 355 (2015) 198–202.
[15] V. Petrillo, et al., PRSTAB 18 (2015) 110701.
[16] A. Bacci, et al., J. Appl. Phys. 113 (2013) 194508.
[17] V. Le Flanchec, P. Balleyguier, J. Treuffet, in: Proceedings of European Particle Accelerator Conference, JACoW, Edinburgh, Scotland, THPCH158, 2006, pp. 3164–3166
[18] J.G. Marmouget, A. Binet, P. Guimbal, J.L. Coacolo, in: Proceedings of European Particle Accelerator Conference, JACoW, Paris, France, 2002, pp 1795–1797
[19] A.S. Chauchat, et al., Nucl. Instrum. Methods A 622 (2010) 129.
[20] T. Suzuki, KEK Report No. KEK-76-3, 1976
[21] P. Guimbal et al., in: Proceedings of European Particle Accelerator Conference, JACoW, Paris, France, 2002, pp 1768–1770